Effects of the Molecular Orientation and Crystallization on Film–Substrate Interfacial Adhesion in Poly(ethylene terephthalate) Film-Insert Moldings

Y. W. Leong, M. Kotaki, H. Hamada

Department of Advanced Fibro Science, Kyoto Institute of Technology, Japan

Received 7 August 2006; accepted 5 October 2006
DOI 10.1002/app.25620
Published online 5 February 2007 in Wiley InterScience (www.interscience.wiley.com).

ABSTRACT: A film and substrate consisting of poly(ethylene terephthalate) were adhered by means of film-insert molding. Two injection speeds (i.e., 50 and 500 mm/s) were chosen to induce different shear rates (and molecular orientation) between the film and the substrate. Annealing was subsequently performed on these specimens at different times and temperatures to examine the extent of orientation-induced crystallization of the substrate surfaces embedded under the film. Differential scanning calorimetry thermograms clearly indicated a shift in the position of the secondary (β) crystalline phase toward a higher temperature in specimens molded at a 500 mm/s injection speed, suggesting that a more densely packed and well-formed crystalline structure was generated because of higher localized orientation of molecules. Polarized Fourier transform infrared spectroscopy analyses provided dichroic ratios of the 1340- and 1410-cm^{-1} wavelengths, which corresponded to the *trans*-glycol conformer and the stable benzene ring, respectively. Drastic increases in the dichroic ratios were observed, especially in specimens molded at a 500 mm/s injection speed after being annealed for 1 min. This could have been caused by the reorientation of molecules fueled by residual stresses, particularly in regions experiencing high shear during molding. © 2007 Wiley Periodicals, Inc. J Appl Polym Sci 104: 2100–2107, 2007

Key words: crystallization; injection molding; interfaces; orientation; polyesters

INTRODUCTION

During the film-insert molding (FIM) process, a technique also known as in-mold decorating, a preprinted film that is formed to the shape of a mold cavity is inserted into the mold, and this is followed by the injection of a melt resin to fill the cavity, which results in a molding consisting of a substrate that is partially wrapped with a decorated film insert. This technique is favored over other conventional methods of surface decoration, that is, silk-screen printing and painting, because it is a one-step decoration process without the need of extra postprocessing facilities that will eventually incur higher production costs. Furthermore, the design is typically reverse-printed on the back of the film so that it is protected from fading by harsh abrasive environments. Nevertheless, good interfacial adhesion between the film and the molded substrate is of immense importance to ensure that the film stays firmly intact to the substrate throughout the lifetime of the product. The interfacial adhesion between two semicrystalline polymers, however, can be influenced by the rate of crystallization, depending on the location of nucleation.[1,2]

In the case of poly(ethylene terephthalate) (PET) FIMs, a high shear rate between the melt resin and film surface could instigate localized orientation of the molecules. There has been extensive interest in the structures and reorganization mechanisms of oriented PET.[3–6] The fact that molecular orientation could induce crystallization of the PET substrate as well as interfacial regions has been widely reported in numerous publications.[7–14] Pereira and Porter[15] attributed the increase in the crystallinity of strain-induced PET to the realignment of the remaining amorphous regions when the polymer is heated above its glass-transition temperature (T_g). Thus, the crystallization process can also be used as a very sensitive probe of chain orientation as well as a powerful rheological property evaluation tool. Interestingly, this reorganization could also significantly affect interfacial adhesion, as shown by these workers.[16,17]

In this study, the influence of interfacial molecular reorganization and crystallization on the film–substrate interfacial properties was evaluated by the subjection of the moldings to isothermal annealing at different temperatures. The slow crystallizing nature of PET allowed us to observe the evolution of interfacial molecular reorganization and crystallinity by annealing the moldings at different time intervals. This

Correspondence to: Y. W. Leong (leongyewwei@hotmail.com).

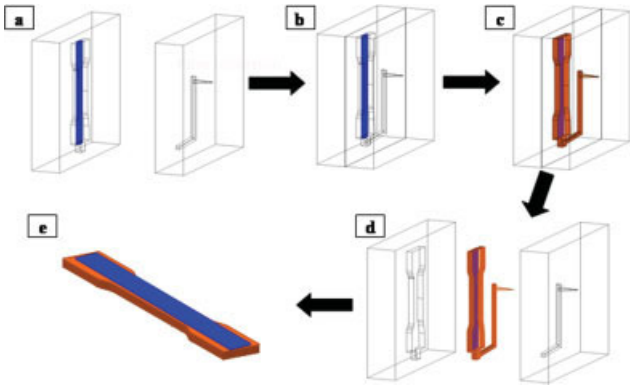

Figure 1 FIM process: (a) film insertion into the mold cavity, (b) mold closing, (c) mold filling, (d) mold opening and extraction of the molding, and (e) final product. [Color figure can be viewed in the online issue, which is available at www.interscience.wiley.com.]

restructuring of the molecules throughout the crystallization process in both the film-insert and control specimens (without film attachment) was monitored through differential scanning calorimetry (DSC) and Fourier transform infrared (FTIR) spectroscopy analyses. Peel tests were performed to gauge the interfacial adhesion properties of the specimens before and after annealing. A molecular model describing the molecular orientation/crystallinity/interfacial property relationship is proposed on the basis of the interpretations and observations of various experimental data.

EXPERIMENTAL

Materials

PET pellets (Bellpet Grade IP123A, supplied by Kanebo Gohshen, Ltd., Osaka, Tokyo, Japan) were dried for 5 h at 120°C to remove moisture before the injection molding. The resin appeared to be highly transparent upon molding and possessed a low melting point (223°C); this suggested that it was a copolymer. The 50-μm-thick PET films (supplied by Toyobo Co., Ltd., Osaka, Tokyo, Japan) that were used as inserts, however, had a higher melting point (251°C), which was consistent with that of neat PET. The films were cut into 174 × 10 mm^2 strips to fit the dumbbell cavity mold. Half the length of the films was adhered to a thin-layer polyimide film, which acted as a nonstick barrier so that these regions could be easily lifted from the substrate after molding and subsequently gripped during the peel test.

Injection molding

Injection molding was carried out at two different injection speeds (i.e., 50 and 500 mm/s) with an ultrahigh-speed injection-molding machine (Po Yuen Machine Fty., Ltd., Hong Kong, P. R. of China) capable of achieving injection speeds up to 1000 mm/s. Each film was inserted into a dumbbell-shaped cavity mold before molding. Upon the injection of the melt resin, heat from the resin was transferred to the film surface, thus causing a certain degree of surface melting and subsequently initiating adhesion. Another set of control specimens was molded, and these were devoid of the film insert for comparison. The FIM cycle is illustrated in Figure 1, whereas the molding conditions are compiled in Table I.

Annealing

The film-insert and control dumbbells were annealed in an oven at two different annealing temperatures, that is, 150 and 200°C. The number of specimens that were placed in the oven was sufficient to allow the retrieval of five specimens at each interval of 1, 5, 10, 30, and 60 min for subsequent characterizations. The annealed specimens were allowed to cool gradually at room temperature before being tested or analyzed.

Infrared spectroscopy and thermal analyses

A PerkinElmer System 2000 (Wellesley, MA) attenuated total reflectance/Fourier transform infrared (ATR–FTIR) spectrometer was used to compare the chemical compositions on the substrate surfaces of both the control and film-insert specimens. The film-insert substrate surface corresponded to the surface that was embedded under the film attachment; thus, the characterization was done only after the film was peeled off the substrate. Scanning was performed in a range of 4000–600 cm^{-1}, with a total of 16 scans under a resolution of 4 cm^{-1} to ensure accuracy. Polarized FTIR spectra were recorded by the fitting of a polarizer inside the optical unit of the analyzer.

DSC analysis (DSC 7, PerkinElmer) was also performed to detect any significant changes in the molecular structure of the surfaces. Specimens were obtained by a thin layer being scraped from the substrate surface with a cutter blade. Thermal scanning was performed at a rate of 10°C/min from 25 to 280°C under a nitrogen atmosphere.

Film–substrate interfacial adhesion characterization and bulk mechanical testing

Because the PET films were relatively thin (50 μm), a 180° peel test was chosen to gauge the interfacial adhesion properties so that the effect of the peeling

TABLE I
Injection-Molding Parameters

Barrel temperature (°C)	280 and 300
Injection speed (mm/s)	50 and 500
Holding pressure (MPa)	250
Mold temperature (°C)	25

angle was negligible. The free end of the film (initially adhered with polyimide tape, which was removed before testing) was gripped to one end of the tensile machine, whereas the part of the substrate that had just been stripped from the film was gripped to the other end. The dimensions and setup of the peel specimens are detailed in Figure 2. The test was conducted at a peeling rate of 5 mm/min with an Instron 4466 universal testing machine (Instron Japan Co., Ltd., Kawasaki, Japan).

The effect of the film insert on the bulk mechanical properties was determined by Charpy impact tests on notched specimens with a universal impact tester (Toyo Seiki Seisaku-Sho, Ltd., Tokyo, Japan). Notches were induced to a depth of 1 mm on the substrate surface first with a notching machine and later with a fresh razor to obtain a sharp notch profile. A 15-J impacter was used, whereas the span length of the specimen was set at 40 mm.

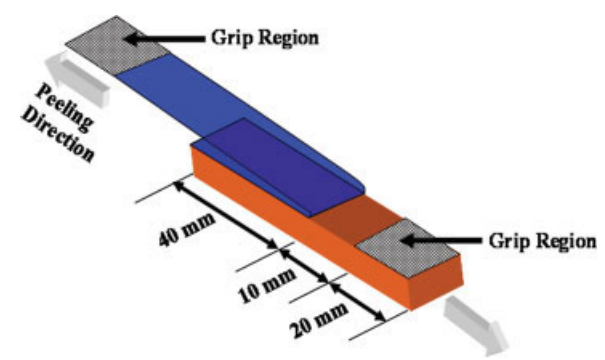

Figure 2 Dimensions of a 180° peel test specimen. [Color figure can be viewed in the online issue, which is available at www.interscience.wiley.com.]

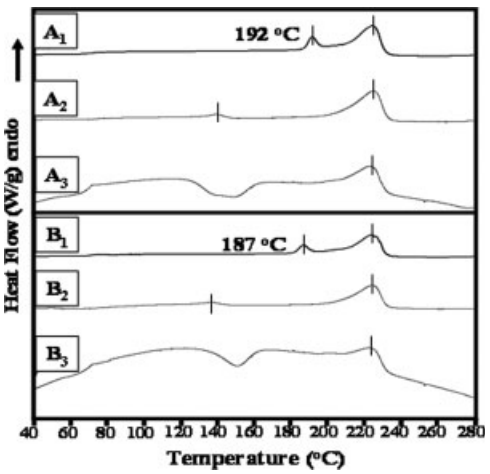

Figure 3 DSC thermograms of annealed specimens molded at a barrel temperature of 280°C and an injection speed of 50 mm/s. A and B represent FIM and control specimens, respectively. Subscripts 1 and 2 denote the specimens annealed at temperatures of 200 and 150°C, respectively, whereas subscript 3 represents unannealed specimens.

RESULTS AND DISCUSSION

Effects of the molding conditions on the crystallization of the annealed FIMs

Among the many annealing temperatures and times that were considered, two annealing temperatures were chosen, that is, 150 (T_{150}) and 200°C (T_{200}), on the basis of the ability of the control specimens to sufficiently crystallize after 1 h of annealing. This was confirmed by the subjection of the specimens to DSC analysis, in which there was no presence of the cold crystallization enthalpy, judging from the thermograms in Figure 3. At both annealing temperatures, the specimens exhibited double enthalpies. The smaller secondary endothermic peak appeared at 140°C, whereas the larger primary peak appeared at 223°C, in specimens annealed at T_{150}. The appearances of the primary and secondary peaks have been attributed to the primary and secondary crystallization processes, respectively, that occur during the isothermal crystallization of PET.[18–21] Primary crystallization takes place during the formation of lamellar structures, which is mainly influenced by the degree of cooling.[18] The progression of growth of these primary lamellar structures would eventually occupy a sizeable bulk volume, which imposes severe restraint on other amorphous regions for the continuous growth of the lamellar stacks. Eventually, the stacking of the primary lamellae would discontinue, whereas the secondary crystallization process would continue to take place, and crystallites with much thinner lamellar structures would form in a discrete manner in residual amorphous regions. Because of the heterogeneous distribution and the thinner lamellar walls, the enthalpies of melting as well as the melting temperatures exhibited by these secondary crystallites are likely to be lower than those of the primary crystallites.

Figure 3(a,b) compares the DSC thermograms of film-insert and control specimens that were left at room temperature (nonannealed) as well as those that were annealed at 200°C (T_{200}) and 150 (T_{150}) for 1 h. These specimens were molded at an injection speed and barrel temperature of 50 mm/s and 280°C, respectively. In all unannealed specimens, the T_g and cold crystallization exotherm are clearly defined, indicating the presence of a substantial amount of amorphous regions due to the fast cooling of these specimens during the molding process. Upon annealing at T_{150}, the definition of T_g was blurred, and the cold crystallization exotherms diminished in both the control and film-insert specimens, whereas a small secondary endotherm appeared around 140°C. At T_{200}, the secondary endotherm shifted to 187 and 192°C in the control and film-insert specimens, respectively. This shift in the secondary endotherm can be attributed to the formation of secondary crystallites with

thicker and denser lamellar structures, which can be achieved through the combination, healing, or perfection of the secondary crystallites when they are given higher thermal energies. The secondary endotherm in the film-insert specimens peaked at a higher temperature than that of the control specimens at T_{200}, and this could be an indication of higher molecular orientation on the film-insert substrates due to the better film–resin interaction versus the resin–mold surface interaction. The primary endotherm constantly peaked at 223°C, regardless of the processing conditions and annealing temperatures.

A more significant change in the thermal characteristics could be observed when the specimens were injected at a higher speed, that is, 500 mm/s, as can be seen in Figure 4. It is apparent that the secondary endotherm peaks for both the control (216°C) and film-insert (218°C) specimens emerged at a much higher temperature than previously demonstrated in Figure 3 when these specimens were annealed at T_{200}. It is thus clear that the injection speed (and ultimately the shear rate) plays an important role in influencing the formation of secondary crystallites. Molecular-orientation-induced crystallization has been known to occur in slow crystallizing polymers such as PET and has received wide coverage.[7–14] Thus, from observations of Figure 4, it can be constructively concluded that the higher injection speed (500 mm/s) could have induced highly anisotropic orientation of the molecules parallel to the flow direction, which were then frozen in place because of subsequent quenching of the resin. Upon annealing, the process of forming the secondary crystallites in the highly oriented region can be smoother and more rapid because of less constraint from the complex amorphous network.

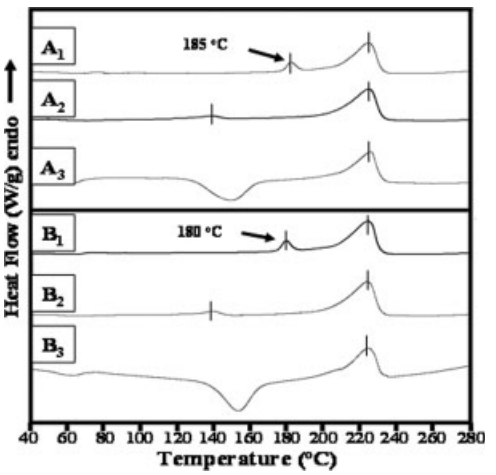

Figure 5 DSC thermograms of annealed specimens molded at a barrel temperature of 300°C and an injection speed of 50 mm/s. A and B represent FIM and control specimens, respectively. Subscripts 1 and 2 denote the specimens annealed at temperatures of 200 and 150°C, respectively, whereas subscript 3 represents unannealed specimens.

Changes in the thermograms could not be observed when the specimens were annealed at T_{150} because this temperature is only bordering the crystallization temperature of PET. Thus, the heat supplied might be able to relieve the molecules from residual stresses and cause minor reorientation (noting the disappearance of the cold crystallization peak), whereas it was insufficient to cause significant recrystallization and lamellar growth.

Similar instances could be seen when comparisons were made of Figures 5 and 6, which present specimens molded at injection speeds of 50 and 500 mm/s, respectively, whereas the barrel temperature was set

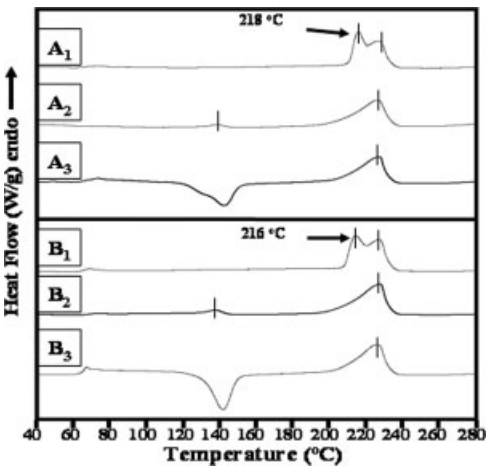

Figure 4 DSC thermograms of annealed specimens molded at a barrel temperature of 280°C and an injection speed of 500 mm/s. A and B represent FIM and control specimens, respectively. Subscripts 1 and 2 denote the specimens annealed at temperatures of 200 and 150°C, respectively, whereas subscript 3 represents unannealed specimens.

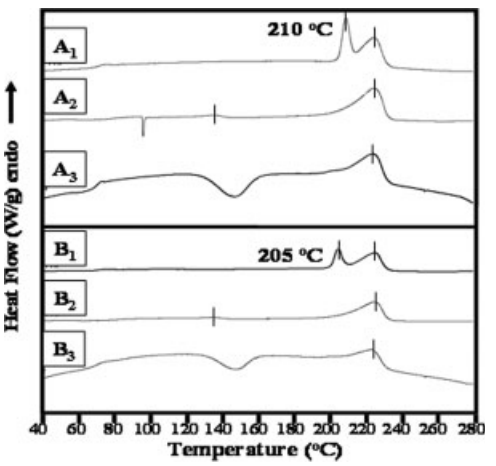

Figure 6 DSC thermograms of annealed specimens molded at a barrel temperature of 300°C and an injection speed of 500 mm/s. A and B represent FIM and control specimens, respectively. Subscripts 1 and 2 denote the specimens annealed at temperatures of 200 and 150°C, respectively, whereas subscript 3 represents unannealed specimens.

at 300°C. However, the secondary peaks exhibited by specimens annealed at T_{200} in Figures 5 and 6 are significantly lower than those of Figures 3 and 4, respectively. Thus, it can be inferred that the state of molecular orientation in specimens molded at 280°C was superior to those molded at a barrel temperature of 300°C. Perhaps the higher viscosity of the resin (at a barrel temperature of 280°C) could have caused higher intermolecular friction, which effected a higher anisotropic orientation of molecules, especially at regions close to the film–resin interface.

Comparisons were also made of the enthalpies (both primary and secondary peaks combined) of the T_{200} specimens and are outlined in Table II. The significant increment in the enthalpies for specimens molded at the 500 mm/s injection speed clearly indicates that higher molecular orientation contributed toward crystal growth in the bulk; similar occurrences have also been noted elsewhere.[15]

State of the molecular orientation and its influence on the crystalline structure

Infrared spectroscopy (ATR–FTIR) was also applied to elucidate the crystallinity at the surface of the substrates to supplement the results from DSC measurements because the former is useful for detecting crystalline structures at a depth of only a few micrometers from the surface while retaining the morphology of the specimens. Hayes et al.[3] also applied the ATR–FTIR technique to elucidate the state of crystallinity of PET by obtaining the area ratios of the 1340-cm^{-1} peak to the 1410-cm^{-1} peak gathered from FTIR spectrographs. Similar ratios were gathered for specimens that were unannealed as well as those annealed for 1, 5, 10, and 30 min at T_{150}; these are plotted in Figures 7 and 8 for film-insert and control specimens, respectively. The annealing temperature of T_{150} was preferred because the relaxation and reorientation rate of the molecules would be much slower, and this allowed us to effectively record the restructuring process throughout the period of annealing.

In the film-insert specimens, the development of the 1340-cm^{-1} band, which is characteristic of the *trans*-glycol conformers, strongly suggests that a significant

TABLE II
Comparison of the Melting Enthalpies Under Different Molding Conditions

Annealing temperature (°C)	Barrel temperature (°C)	Injection speed (mm/s)	Melting enthalpy (J/g)
200	280	50	37.02
		500	39.26
	300	50	34.03
		500	44.76

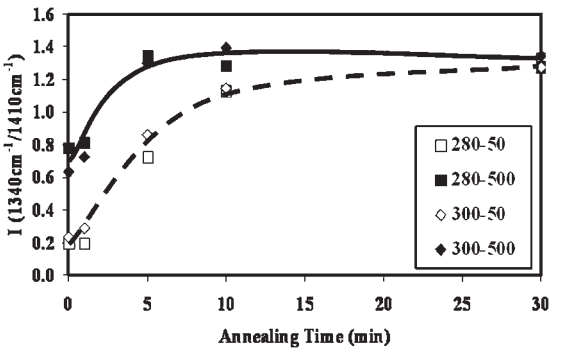

Figure 7 Development of the 1340 cm^{-1}/1410 cm^{-1} FTIR band ratios throughout the period of annealing in FIMs prepared at barrel temperatures of 280 and 300°C and injection speeds of 50 and 500 mm/s. The legend should be read as the barrel temperature minus the injection speed.

increment in the crystallinity was apparent in all specimens, regardless of the injection speeds at the end of the annealing process. Although the 1340 cm^{-1}/1410 cm^{-1} ratios congregated toward the end of the annealing process, the rate of conformational changes differed in the initial stages of annealing, especially when the specimens were molded at different injection speeds. Film-insert specimens molded at a higher injection speed (500 mm/s) underwent a more substantial crystallization than specimens molded at lower injection speeds (50 mm/s). This phenomenon could confirm the earlier assumption that the presence of high molecular orientation at the film–substrate interfacial regions in specimens molded at high injection speeds could strongly induce crystallization.

The surface crystallinity of the control specimens seemed to have also increased with the annealing time, judging from the rise in the 1340 cm^{-1}/1410 cm^{-1} ratios in Figure 8, although there was no apparent difference in terms of conformational changes when the injection speed was varied. It is important to recall that the FTIR beam penetrates to a depth of

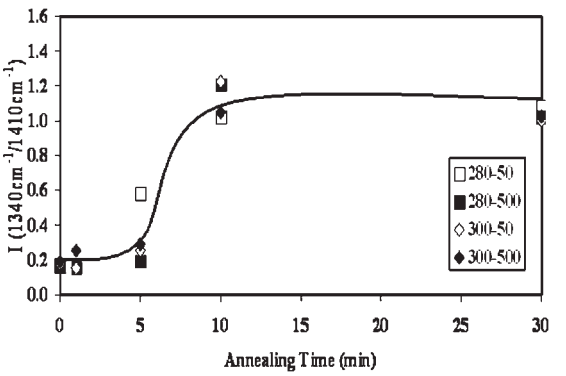

Figure 8 Development of the 1340 cm^{-1}/1410 cm^{-1} FTIR band ratios throughout the period of annealing in control specimens prepared at barrel temperatures of 280 and 300°C and injection speeds of 50 and 500 mm/s. The legend should be read as the barrel temperature minus the injection speed.

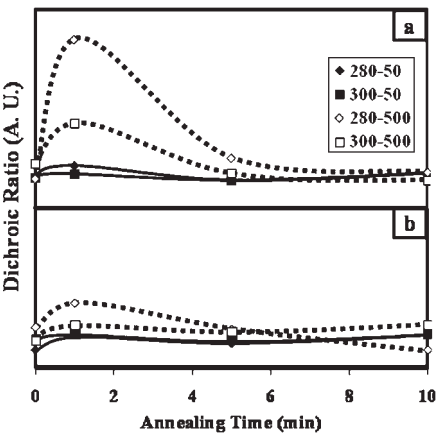

Figure 9 Molecular orientation reflected through the dichroic ratio of the inner substrate surfaces for the first 10 min of annealing in (a) FIMs and (b) control specimens. The legend should be read as the barrel temperature minus the injection speed.

only a few micrometers of the specimen surface, which most likely includes a layer of frozen skin consisting of randomly oriented chains. Any form of molecular orientation would lie under this skin region. The thickness of this skin layer is greatly dependent on the temperature gradient between the melt resin and the film (in the case of film-insert specimens) or the mold surface (in the case of control specimens). Because the temperature gradient between the resin and mold surface is expected to be higher, the skin layer in control specimens is likely to be thicker. During annealing, the structural changes induced by the restructuring of oriented molecules would also likely affect the structure of the surrounding regions, including a certain depth of the skin. However, because of the thick skin layer in the control specimens, these structural changes could not be detected on account of the low penetration of the FTIR beam. On the contrary, the effect of the injection speed on the restructuring of molecules was detectable in the film-insert specimens, and this could be due to the presence of a comparatively much thinner skin layer that posed less hindrance to the FTIR incidence beam. It is also possible that the state of molecular orientation in the film-insert specimens was superior to that of the control because the film–resin interaction was higher than that between the resin and the mold surface.

The orientation of the *trans*-glycol conformers could be determined with a polarizer during the ATR–FTIR measurements to obtain the intensity of the 1340-cm^{-1} band when the specimens were placed parallel and perpendicular to the polarizer. The ratios of the parallel and perpendicular intensities, also known as the dichroic ratios,[14] were then plotted for the film-insert and control specimens in Figure 9(a,b), respectively. Before annealing, the substrate surfaces did not exhibit any preferential dichroism, even in the film-insert specimens. This indicates that the outermost surfaces of the substrate consist of a nonoriented skin layer that forms during the fast cooling of the moldings. Upon annealing, however, the state of orientation of the surfaces may change, depending on the extent of orientation and also the thickness of the skin layer. In the film-insert specimen, the skin layer was considered to be very thin because of the lower cooling rate caused by the hindrance of heat transfer by the film. Hence, the highly oriented regions could be situated very close to the surface directly under the skin. Upon annealing, these regions reorganized almost instantaneously, thus affecting the structures of the skin regions as well, and this explains the emergence of the dichroic peaks parallel to the flow direction after only 1 min of annealing, as can be seen in Figure 9(a). Nevertheless, this occurred only in specimens molded at the 500 mm/s injection speed, whereas those molded at 50 mm/s had very minimal or no changes in dichroism. Upon further annealing, the dichroism decayed as the crystallization and relaxation of the molecules took place.

Similar observations could not be detected in control specimens, as shown in Figure 9(b), for which most of the recorded dichroism peaks were very weak when compared with those of film-insert specimens. This again underscores the initial suggestion that the oriented regions were located far from the surface of the substrate because of the formation of a thick skin layer in the control specimens.

Effects of annealing on the film–substrate adhesion

The effects of the annealing time and 1340 cm^{-1}/1410 cm^{-1} ratios on the film–substrate adhesion of FIMs are considered in Figures 10 and 11, respectively. The peel strength decreased with an increase in the 1340 cm^{-1}/1410 cm^{-1} ratios (crystallinity) and annealing

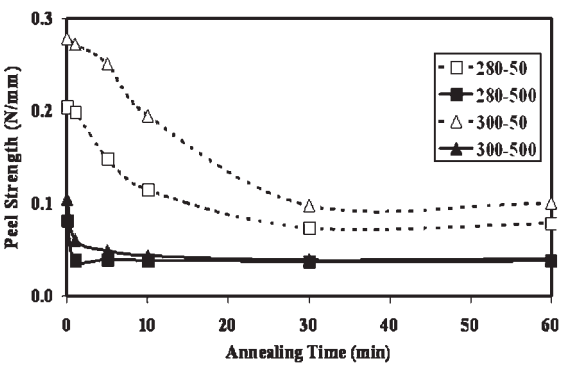

Figure 10 Relationship between the peel strength and annealing time for FIMs. The legend should be read as the barrel temperature minus the injection speed.

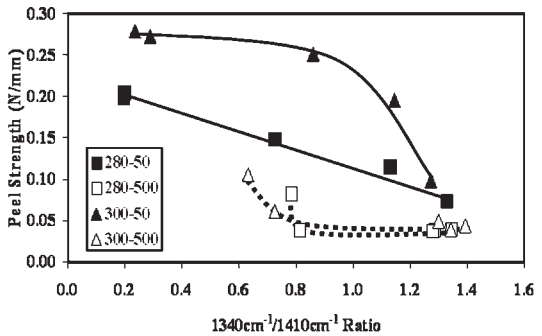

Figure 11 Relationship between the peel strength and the 1340 cm^{-1}/1410 cm^{-1} ratio. The legend should be read as the barrel temperature minus the injection speed.

time in all the specimens; the severity depended on the speed at which these specimens were molded. Generally, specimens molded at lower injection speeds experienced a more gradual descent in the peel strength with the annealing time and most likely retained a higher peel strength at the end of the annealing stage. Specimens that were molded at higher injection speeds incurred a greater reduction of the peel strength, which was most drastic in the initial stages of annealing, in which sudden conformational changes occurred. All these indications provide a clear understanding that the crystallization and reorientation of molecules in the PET substrate could severely disrupt film–substrate interactions.

The molecular models in Figure 12 represent the sequence of molecular motion and entanglement during annealing. Figure 12(A_1) shows a model with a high density of molecular entanglements at the interfacial region that could ideally provide good interfacial bonding between the film and substrate. Because the melt flow of PET is quite high, good contact between the PET resin and film surface can be easily attained even at the lowest barrel temperature used in this study (280°C). Higher barrel temperatures would not only create more free and energetic molecules in the resin but also increase the temperature gradient between the resin and film surfaces. This allows higher molecular interactions at the film–substrate interface that are subsequently quenched, thus leaving a highly amorphous interfacial region with excellent retention of molecular entanglement.

Apart from the temperature, the effects of the resin injection speed were often related to the state of molecular orientation in the interfacial regions. The extent of molecular orientation in the interfacial regions at different injection speeds is compared in Figure 12(A_1,B_1). The low injection speed encouraged random orientation of the molecules because less shear-induced stretching was sustained by these molecules. In this relaxed state, the molecules from the substrate could navigate more freely across the interface to form more entanglements with molecules from the film, which subsequently generated strong bonding. In high-injection-speed-molded specimens, the molecules oriented anisotropically toward the flow direction, thus hindering interaction between the main molecular chains from the substrate and the film. In this case, the entanglements at the interface were believed to be generated from mostly short chains or branches extended from the main chains, which provided very weak anchorage and bonding across the interface.

The annealing of PET FIMs has provided great understanding of the state of substrate molecular orientation, the effects on crystal growth, and most importantly, the competition between crystallization and entanglement at the interfacial region. The schematic models in Figure 12(A_2,B_2) suggest the evolution of crystal growth during annealing in specimens molded at different injection speeds. During the crystallization process, the molecules tend to realign and fold themselves into lamellar structures, so there could be a lower volume of loose molecules that could form effective entanglements as crystallization proceeds. In low-injection-speed specimens, the rate of crystallization during the annealing process will be lower because the more relaxed and less ordered state of the molecules does not favor high crystallization rates. In this case, there could still be large volumes of free molecules that remain as entanglements at the interfaces at the end of the annealing process. On the other hand, in high-injection-speed-molded specimens, the stored stresses in the highly stretched molecules will be released when the glass transition of the material is reached. Because of the momentum of stress release, the folding of molecules could occur almost instantaneously to form lamellar structures,

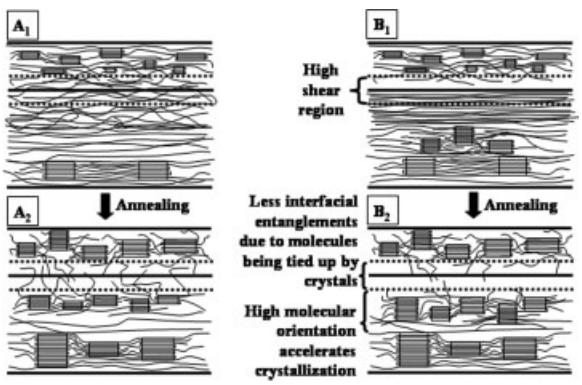

Figure 12 Schematic model indicating the evolution of crystallization and its effect on interfacial entanglement during the annealing of specimens molded at different injection speeds. Specimens molded at low and high injection speeds are represented by schematics A and B, respectively. Subscripts 1 and 2 indicate the specimens before and after annealing, respectively.

while simultaneously depleting the volume of free molecular strains at the interfacial regions. This is thought to have effectively caused the significant reduction in interfacial adhesion in the high-injection-speed-molded specimens upon annealing.

CONCLUSIONS

FIMs were produced with different injection speeds and barrel temperatures. Annealing was subsequently performed on these specimens at different times and temperatures to examine the extent of orientation-induced crystallization of the substrate surfaces embedded under the film. A shift in the secondary crystallization endotherm was observed in the DSC thermograms of specimens molded at different injection speeds, thus suggesting that various injection speeds could induce different formations of crystallites. The secondary endotherm in high-injection-speed specimens appeared at higher temperatures, indicating a smoother molecular restructuring process, which produced thicker and denser lamellar structures upon annealing. This was thought to be possible only when the molecules were highly oriented, which could provide less hindrance during the restructuring process. This high molecular orientation was detected in the FTIR spectra, which also provided evidence that the film–resin interaction was much stronger than the resin–mold surface interaction. High molecular orientation and crystallization rates were touted to be detrimental toward the film–substrate adhesion properties. Molecular models suggest that regions that are highly oriented possess fewer free molecules that can interact and form entanglements across the interface, thus causing weak interfacial adhesion. During the annealing process, the molecules of these regions could also induce crystallization, which would also tie down the molecules, thus preventing any substrate molecules from interacting with the film.

References

1. Boucher, E.; Folkers, J. P.; Creton, C.; Hervet, H.; Leger, L. Macromolecules 1997, 30, 2102.
2. Lo, C. T.; Laabs, F. C.; Narasimhan, B. J Polym Sci Part B: Polym Phys 2004, 42, 2667.
3. Hayes, N. W.; Beamson, G.; Clark, D. T.; Law, D. S.-L.; Raval, R. Surf Interface Anal 1996, 24, 723.
4. Miyake, A. J Polym Sci 1959, 38, 479.
5. Farrow, G.; Ward, I. M. Polymer 1960, 1, 330.
6. Lin, S. B.; Koenig, J. L. J Polym Sci Polym Phys Ed 1982, 20, 2277.
7. Ben Daly, H.; Sanschagrin, B.; Nguyen, K. T.; Cole, K. C. Polym Eng Sci 1999, 39, 1736.
8. Ben Daly, H.; Cole, K. C.; Sanschagrin, B.; Nguyen, K. T. Polym Eng Sci 1999, 39, 1982.
9. Rueda, D. R.; Kubera, L.; Balta-Calleja, F. J.; Bayer, R. K. J Mater Sci Lett 1993, 12, 1140.
10. Duchesne, C.; Kong, X.; Brisson, J.; Pezolet, M.; Prud'homme, R. E. Macromolecules 2002, 35, 8768.
11. Blundell, D. J.; Oldman, R. J.; Fuller, W.; Mahendrasingam, A.; Martin, C.; MacKerron, D. H.; Harvie, J. L.; Riekel, C. Polym Bull 1999, 42, 357.
12. Salem, D. R. Polym Eng Sci 1999, 39, 2419.
13. Karim Oultache, A.; Kong, X.; Pellerin, C.; Brisson, J.; Pezolet, M.; Prud'homme, R. E. Polymer 2001, 42, 9051.
14. Radhakrishnan, J.; Kaito, A. Polymer 2001, 42, 3859.
15. Pereira, J. R. C.; Porter, R. S. J Polym Sci 1983, 21, 1147.
16. Shibayama, M.; Izutani, A.; Ishikawa, A.; Tanaka, K.; Nomura, S. Polymer 1994, 35, 271.
17. Mueller, C.; Capaccio, G.; Hiltner, A.; Baer, E. J Appl Polym Sci 1998, 70, 2021.
18. Wang, Z.-G.; Hsiao, B. S.; Sauer, B. B.; Kampert, W. G. Polymer 1999, 40, 4615.
19. Medellin-Rodriguez, F. J.; Lopez-Guillen, R.; Waldo-Mendoza, M. A. J Polym Sci Part B: Polym Phys 1999, 37, 1981.
20. Medellin-Rodriguez, F. J.; Phillips, P. J.; Lin, J. S.; Campos, R. J Polym Sci Part B: Polym Phys 1997, 35, 1757.
21. Tan, S.; Su, A.; Li, W.; Zhou, E. Macromol Rapid Commun 1998, 19, 11.